Korean J. Chem. Eng., **24**(5), 774-780 (2007)

Effect of Pt addition on vanadium-incorporated TiO_2 catalysts for photodecomposition of ammonia

Min-Kyu Jeon and Misook Kang*,†

Production, Johnson Matthey Catalysts Korea, Hwaseong, Gyeonggi 445-940, Korea
*Department of Chemistry, College of Science, Yeungnam University, Gyeongsan, Gyeongbuk 712-749, Korea
(*Received 27 February 2007 • accepted 17 May 2007*)

Abstract−This study investigated the effect of adding Pt components to V-TiO_2 for highly concentrated ammonia photodecomposition. Pt components were introduced to the V-TiO_2 photocatalysts by using two method types: the common sol-gel (Pt-V-TiO_2) and impregnation (Pt/V-TiO_2) methods. The observed X-ray diffraction (XRD) peaks were assigned to V_2O_5 at 19.5, 27.5 and 30.20° in V-TiO_2, and to Pt metals at 39.80° (111) in Pt/V-TiO_2. The Pt component of Pt-V-TiO_2 was identified as Pt^{2+} from the $Pt4f_{7/2}$ and $Pt4f_{5/2}$ bands at 73.6 and 77.4 eV in XPS bands, respectively, but the band was shifted to a lower binding energy in Pt/V-TiO_2. The H_2 temperature-programmed reduction (TPR) curves showed that the temperature of reduction from Ti^{3+} to Ti^0 was decreased by Pt addition and that the area was larger in Pt-V-TiO_2 than in Pt/V-TiO_2. The NH_3 decomposition was slightly increased with vanadium addition compared to that of pure TiO_2, and the decomposition was further enhanced with Pt addition. Particularly, the NH_3 (1,000 ppm) decomposition reached 100% over Pt/V-TiO_2 after 120 min, although about 10-30% of the ammonia was converted into undesirable NO_2 and NO.

Key words: Pt/V-TiO_2, Pt-V-TiO_2, NH_3 Photodecomposition

INTRODUCTION

Ammonia is a serious wastewater pollutant that induces the eutrophication of rivers and lakes [1,2], and its odor is also detrimental to humans. Because the importance of removing ammonia has increased, it is treated using biological techniques, adsorption, and thermal incineration. Recently, the catalytic decomposition of ammonia in wastewater using metal-TiO_2 photocatalysts has attracted much attention [3-6]. Most researchers have focused on transforming all ammonia molecules into N_2 via the following photocatalytic redox reaction: $4\ NH_3+3\ O_2 \rightarrow 2\ N_2+6\ H_2O$. However, it has been reported that when metal-incorporated TiO_2 photocatalysts are used to decompose ammonia, considerable amounts of NO, NO_2, and HNO_3 are formed. Consequently, new photocatalysts are needed to eliminate NO_x compounds which cause secondary contamination. Previously, we attempted to introduce V-TiO_2 for the photodecomposition of methyl orange, which has a nitrogen component [7]. We discovered that the addition of vanadium to the TiO_2 framework improved the photodecomposition of nitrogen compounds compared to that of pure TiO_2.

The main objective of this study was to enhance the photocatalytic decomposition of ammonia, by transforming NH_3 into N_2. We produced pure TiO_2, V-TiO_2, Pt-V-TiO_2, and Pt/V-TiO_2 photocatalysts using two methods: sol-gel and impregnation. To confirm the relationship between the physical properties of the photocatalysts and their catalytic decomposition of NH_3, the four types of photocatalyst were analyzed by X-ray diffraction (XRD), X-ray photoelectron spectroscopy (XPS), UV-visible spectra, hydrogen temperature-programmed reduction (H_2-TPR), and ammonia temperature-programmed desorption (NH_3-TPD).

†To whom correspondence should be addressed.
E-mail: mskang@ynu.ac.kr

EXPERIMENTAL

1. Preparation of TiO_2, V-TiO_2, Pt-V-TiO_2, and Pt/V-TiO_2 Photocatalysts

TiO_2 and 5.0 mol% V-TiO_2 photocatalysts were prepared by using a conventional, sol-gel method to insert vanadium into the TiO_2 framework, as shown in Fig. 1a and b. To prepare the sol mixture,

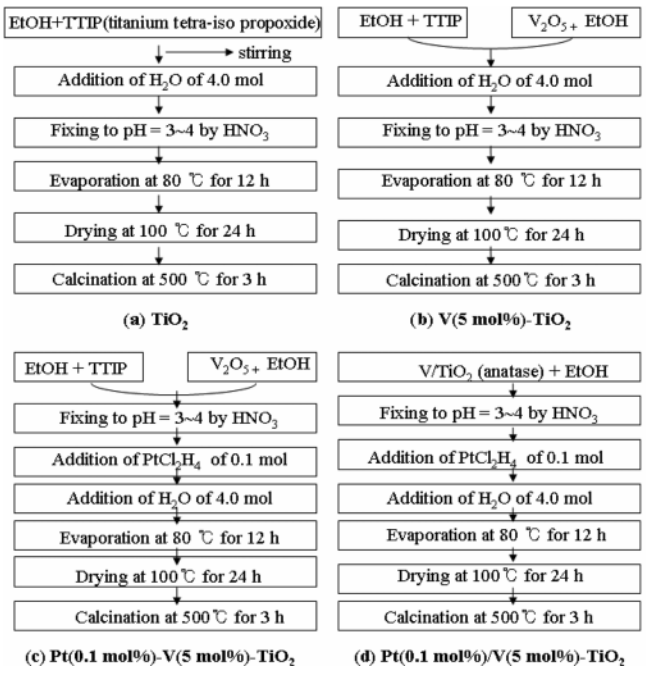

Fig. 1. Preparation of nanometer-sized TiO_2, V-TiO_2, Pt-V-TiO_2, and Pt/V-TiO_2 photocatalysts using sol-gel and impregnation methods.

titanium tetraisopropoxide (TTIP, 99.95%, Junsei Chemical, Tokyo, Japan) and vanadium chloride (99.9%, VCl_5; Junsei Chemical) were used as the titanium and vanadium precursors, respectively, and ethanol (Wako Pure Chemical, Osaka, Japan) was used as the solvent. To 100 ml of ethanol were added 0.1 mol TTIP and 5.0 mol% VCl_5, after which 0.4 mol distilled water was added to induce hydrolysis. Simultaneously, for the preparation of Pt-V-TiO_2, 1.0 wt% $PtCl_2H_4$ (99.9%; Aldrich, Milwaukee, WI, USA) was added to the final solution, as shown in Fig. 1c. Finally, the solution was adjusted to pH= 3.0. TTIP and VCl_5 were hydrolyzed via the OH group during evaporation at 80 °C for 12 h. The resulting yellowish precipitate was dried at 100 °C for 24 h, and then heated at 500 °C for 3 h to form the anatase structure. For Pt/V-TiO_2, the prepared V-TiO_2 was impregnated with Pt precursor, as shown in Fig. 1d. To the V-TiO_2 powders and ethanol prepared above, 1.0 wt% $PtCl_2H_4$ (99.9%; Aldrich, Milwaukee, WI, USA) was added. The ethanol was removed by evaporation at 80 °C for 12 h, and the mixture was dried and calcined at 500 °C for 3 h to obtain crystallized Pt/V-TiO_2 photocatalyst.

2. Characterizations of TiO_2, V-TiO_2, Pt-V-TiO_2, and Pt/V-TiO_2 Photocatalysts

The synthesized four powders (TiO_2, V-TiO_2, Pt-V-TiO_2, and Pt/V-TiO_2) were subjected to XRD (model PW 1830; Philips, Amsterdam, The Netherlands) with nickel-filtered CuKα radiation (30 kV, 30 mA) at 2θ angles ranging from 5 to 70 °.

The sizes and shapes of the four particles were observed with scanning electron microscopy (SEM, model JEOL-JSM35CF; Tokyo, Japan). The power was set to 15 kV.

UV-visible spectra of the four powders were obtained by using a Shimadzu MPS-2000 spectrometer (Kyoto, Japan) with a reflectance sphere. The special range was from 200 to 800 nm.

XPS measurements of Pt4f, V2p, Ti2p, and O1s were recorded with an ESCA 2000 (VZ MicroTech, Oxford, UK) system equipped with a non-monochromatic AlKα (1486.6 eV) X-ray source. The four powders were pelletized at 1.2×10^4 kPa for 1 min, and then the 1.0-mm pellets were maintained in a vacuum (1.0×10^{-7} Pa) overnight to remove water molecules from the surface before the measurement. The base pressure of the ESCA system was below 1×10^{-9} Pa. Experiments were recorded with 200-W source power and an angular acceptance of ±5 °. The analyzer axis made an angle of 90 ° with the specimen surface. Wide scan spectra were measured over a binding energy range of 0 to 1,200 eV and pass energy of 100.0 eV. The Ar^+ bombardment of the four powders was performed with an ion current of 70 to 100 nA over an area of 10.0×10.0 mm and the total sputter time was 2,400 s divided into 60 intervals. A Shirley function was used to eliminate the background in the XPS data analysis. The XPS signals of O1s, Ti2p, Pt4f, and V2p were fitted by using mixed Lorentzian-Gaussian curves.

NH_3-TPD measurements of the four powders were carried out on a conventional TPD system equipped with a TCD cell. The catalysts were exposed to He gas at 550 °C for 2 h in order to remove water and impurities on surface. After pretreatment, the samples were exposed to ammonia for 1 h and then were heated to 700 °C at a rate of 10 °C/min. The amount of desorbed gas was continuously monitored with a TCD cell. About 3.0 g of the catalyst sample was loaded in a quartz reactor, heated at 200 °C for 6 h, and then cooled down to room temperature (RT) in He gas condition.

H_2-TPR was performed next. About 0.3 g of each of the four powders was pretreated under He flow (30 mL/min) at 550 °C for 2 h, and then cooled to RT. Analysis was carried out by flowing 30 mL/min of H_2 (10 vol-percent)/N_2 and raising the catalyst temperature from RT to 550 °C at 5 °C/min. The change in hydrogen concentration was measured with a gas chromatograph (GC series 580, GOW-MAC) equipped with a TCD.

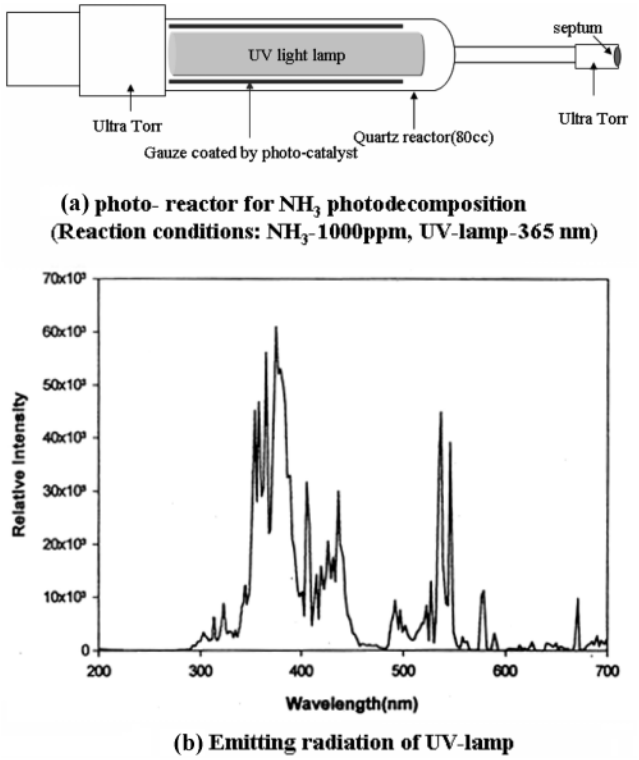

Fig. 2. Schematic of gas-phase batch reactor for NH_3 removal and wavelengths emitted from UV-lamp. Reaction conditions: UV-lamp, 4ea (4 W/cm², 365 nm); NH_3, 1,000 ppm; reaction time, 3 h; catalyst coated on glass bead, 1.0 g.

3. Analysis of Ammonia Decomposition over TiO_2, V-TiO_2, Pt-V-TiO_2, and Pt/V-TiO_2 Photocatalysts

Ammonia was decomposed by using a gas-phase batch system, as shown in Fig. 2a. A quartz cylinder reactor (30 cm long and 1.0 cm in diameter) was used, and UV-lamps (model BBL, 365 nm, 4ea×6 W/m², 20 cm long×1.5 cm in diameter; Shinan, Sunchun, Korea) were used for the photoreaction and the emitted wavelength, as shown in Fig. 2b. The photocatalysts were coated on a gauze as a support by using a dipping method, as shown Fig. 3a, after which the gauze was thermal-pressed at 250 °C (Fig. 3b). The amount of catalyst coating was fixed at 1.0 g and the concentration of ammonia added to the batch system was fixed at 1,000 ppm.

The ammonia concentrations before and after photodecomposition were analyzed by gas chromatography (GC17A; Shimadzu, Kyoto, Japan) with flame-ionization/thermal-conductivity detectors (FID/TCD) (HP-1 capillary column). The percentage removed was calculated from the disappearance of the pollutant during the decomposition process. All experiments were performed at RT and atmospheric pressure. FT-IR spectrometry (FTIR-8400; Shimadzu) and GC/MS were used to quantify the products after ammonia decomposition at a reaction time of 60 min.

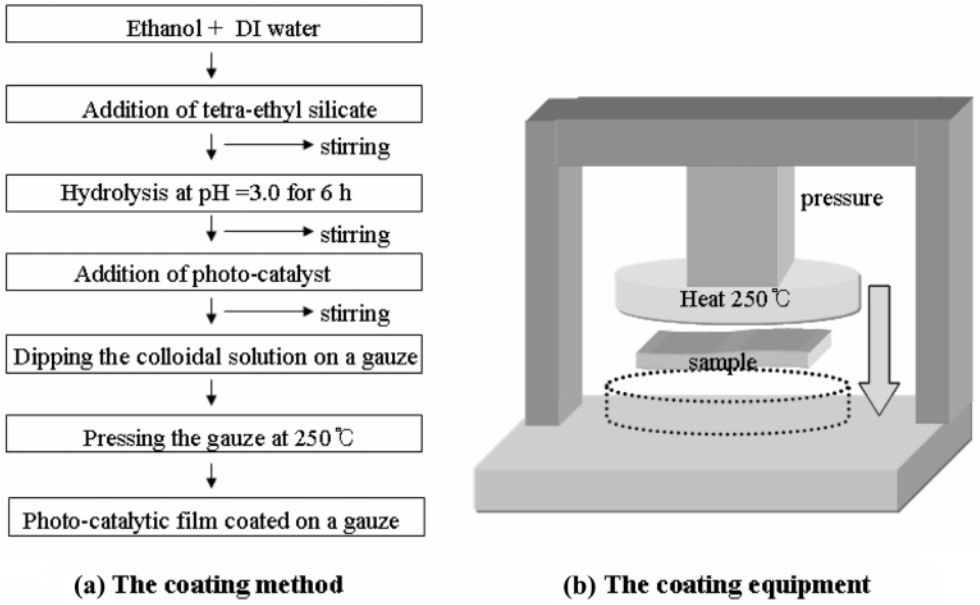

Fig. 3. Fixation of nanometer photocatalyst particles on gauze by using a dipping method.

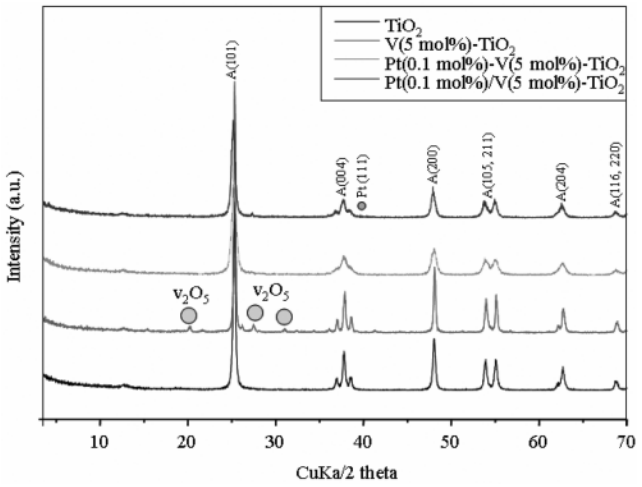

Fig. 4. XRD pattern of nanometer-sized TiO_2, V-TiO_2, Pt-V-TiO_2, and Pt/V-TiO_2 photocatalysts.

RESULTS AND DISCUSSION

1. Characteristics of the TiO_2, V-TiO_2, Pt-V-TiO_2, and Pt/V-TiO_2 Photocatalysts

Fig. 4 shows the XRD patterns of the four photocatalysts. Photocatalytic TiO_2 with an anatase structure was used to decompose the volatile organic compounds. All the samples had a well-developed anatase structure (symbol A). However, the peak was weaker with Pt addition than with pure TiO_2 and V-TiO_2 addition, and the peaks were particularly broader in Pt-V-TiO_2. Generally, the broader the peaks, the smaller the crystallites are. A peak assigned to V_2O_5 (010) appeared at around 2θ=19.5, 27.5, 30.20° for V-TiO_2, but not for the other catalysts. In addition, a peak for Pt (111) metal at 2θ=39.80° was also seen for only the Pt-impregnated sample, although the Pt oxide components could not be determined in the XRD analysis.

SEM photographs of the four photocatalysts are shown in Fig. 5. The shape of all the catalysts was relatively uniform and spherical. The pure TiO_2 particles were the smallest, and the particle size increased with vanadium addition, and increased further with platinum impregnation. However, the size was smallest in Pt-V-TiO_2. These results matched the XRD result in Fig. 4.

Table 1 summarizes the real atomic compositions of the four photocatalysts calculated from the energy dispersive analysis of X-rays (EDAX). The true atomic percentage of vanadium/titanium was 0.14, 0.05, and 0.05 in V-TiO_2, Pt-V-TiO_2, and Pt/V-TiO_2, respectively. Unfortunately, due to the undetectable amount and high dispersion over V-TiO_2, we could not determine the Pt component in Pt-V-TiO_2 by the EDAX results.

We performed an XPS analysis of Ti2p, O1s, V2P, and Pt4f on the four particles, as shown in Fig. 6. The $Ti2p_{1/2}$ and $Ti2p_{3/2}$ spin-orbital splitting photoelectrons for anatase TiO_2 were located at binding energies of 463.7 and 458.5 eV, respectively, and were assigned to the presence of typical Ti^{4+}, although the band was shifted to a higher binding energy for TiO_2. The bands were broadened when V was added, and shifted markedly to a higher binding energy at 458.1 eV for $Ti2p_{3/2}$. However, this band was restored with Pt addition. In general, a high binding energy indicates that the metal has a high valence. Conversely, the measured full width at half maximum (FWHM) of the $Ti2p_{3/2}$ peak increased with Pt addition, and this tendency was the largest in Pt/V-TiO_2. A greater FWHM usually indicates an increased amount of less-oxidized metals [8]. Gaussian fitting was used in the curve resolutions of the O1s peaks (first peak: 529.5, second peak: 531.4 eV) in the two spectra, which were assigned to metal-O and metal-OH, respectively. The two separate peaks were shifted remarkably to a higher binding energy in the order of TiO_2<V-TiO_2<Pt-V-TiO_2=Pt/V-TiO_2. Nevertheless, the ratio of metal-OH/metal-O in the O1s peaks decreased in the order of Pt/V-TiO_2>Pt-V-TiO_2>TiO_2>V-TiO_2. A higher metal-OH peak generally indicates that the particles are more hydrophilic [9,10]. In contrast, the measured FWHM of the O1s peak was the largest in

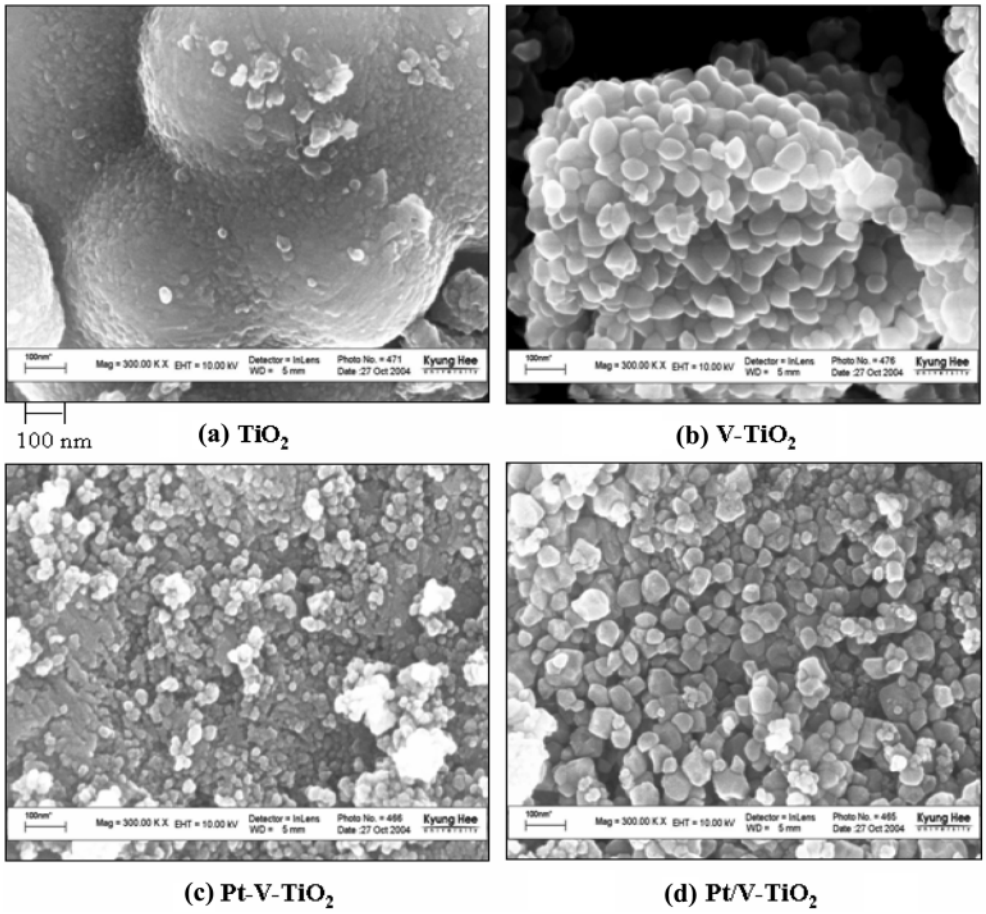

Fig. 5. SEM photographs of nanometer-sized TiO_2, V-TiO_2, Pt-V-TiO_2, and Pt/V-TiO_2 photocatalysts.

Table 1. Real atomic compositions of nanometer-sized TiO_2, V-TiO_2, Pt-V-TiO_2, and Pt/V-TiO_2 photocatalysts

Photocatalyst	Weight %				Atomic %			
	O	Ti	V	Pt	O	Ti	V	Pt
Pure TiO_2	39.55	60.45			66.20	33.80		
V(5 mol%)-TiO_2	31.63	61.99	6.38		55.98	38.32	5.69	
Pt(0.1 mol%)-V(5 mol%)-TiO_2	33.75	62.90	3.36	-	60.47	37.64	1.89	-
Pt(0.1 mol%)-V(5 mol%)-TiO_2	29.43	66.97	3.60	-	55.51	42.35	2.14	-

V-TiO_2, similar to the tendency for the FWHM of the Ti2p peaks. Conversely, the bands assigned to $V2p_{3/2}$ (517.9 eV) and $V2p_{1/2}$ (524.8 eV) in the V^{5+} oxide (V_2O_5) appeared on V-TiO_2, Pt-V-TiO_2, and Pt/V-TiO_2, while the band was shifted to the lowest binding energy with Pt impregnation, which indicates a lower metal valence state. Moreover, the FWHMs were larger in Pt-V-TiO_2 and Pt/V-TiO_2. From the XPS results for Ti2p and V2P, we confirmed that the Ti and V ions are reduced with platinum addition and, in particular, by Pt impregnation. Furthermore, we had already determined that the binding energies for the Pt4f orbital to the four peaks at 80.0, 77.0, 73.0, and 70.0 eV were assigned to Pt $4f_{5/2}$, PtO $4f_{5/2}$, PtO $4f_{7/2}$, and PtO_2 $4f_{7/2}$, respectively [11]. Therefore, the Pt $4f_{7/2}$ (73.6 eV) and Pt $4f_{5/2}$ (77.5 eV) bands confirmed that the Pt component in Pt-V-TiO_2 existed as PtO. These bands in Pt/V-TiO_2 were shifted to a lower binding energy, which indicated a low oxidation state.

Fig. 7 shows the UV-visible spectra of the four particles. The absorption of Ti^{4+} tetrahedral symmetry normally appears around 350 nm. In the figure, the absorption band was around 360 nm in pure TiO_2, but was shifted to a higher wavelength in the V-TiO_2 and Pt-TiO_2 than in pure TiO_2. Surprisingly, the photocatalysts absorbed all wavelengths from 200 to 800 nm with Pt addition, and especially so in Pt-V-TiO_2. Generally, the band gaps in a semiconductor material are closely related to the wave range absorbed. The higher the absorption wavelength, the shorter the band gap is. The red shift of absorption band by addition of V and Pt ions may be attributable to the transition metals having more d orbital electrons; the absorption band by d-d transfer is shown at longer wavelength in UV-visible range. Here, V and Pt ions have more d orbital electrons than that in Ti ion. Therefore, we postulated that Pt addition lowered the band gap energy, and that consequently the photocata-

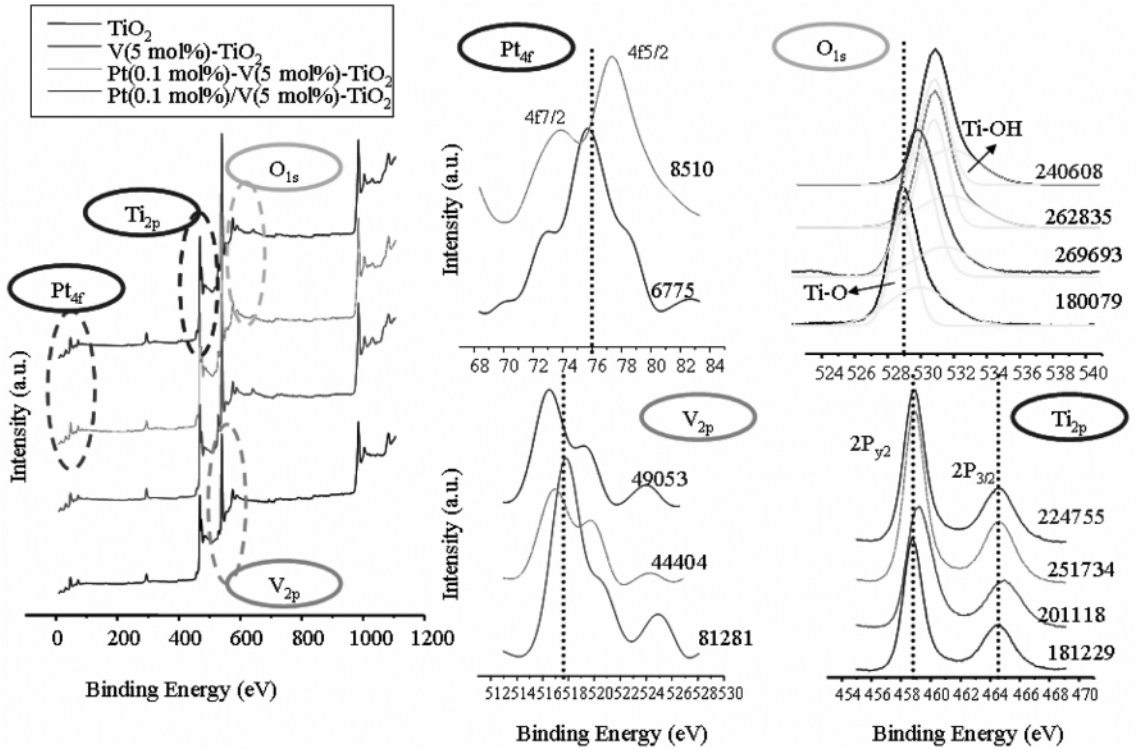

Fig. 6. XPS spectroscopy results for O1s, Pt4f, Ti2p, and V2P, of nanometer-sized TiO_2, V-TiO_2, Pt-V-TiO_2, and Pt/V-TiO_2 photocatalysts.

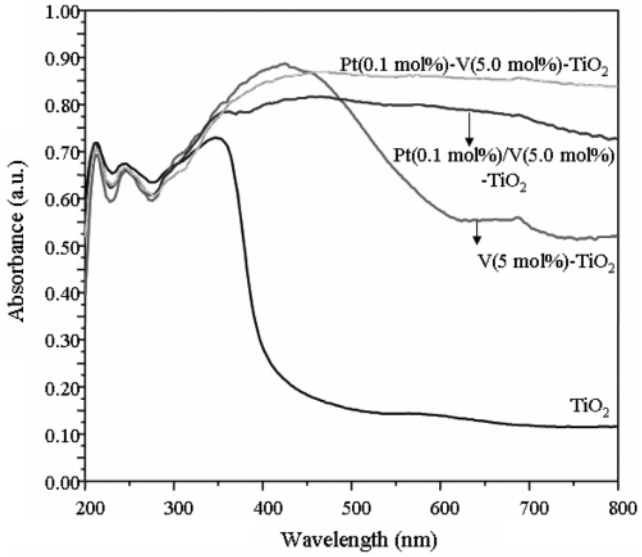

Fig. 7. UV-visible spectra of nanometer-sized TiO_2, V-TiO_2, Pt-V-TiO_2, and Pt/V-TiO_2 photocatalysts.

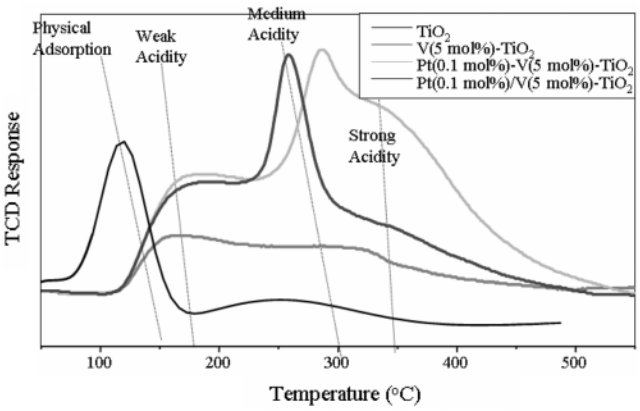

Fig. 8. NH_3-TPD profiles of nanometer-sized TiO_2, V-TiO_2, Pt-V-TiO_2, and Pt/V-TiO_2 photocatalysts.

lysts could be activated at a weak energy, like that of visible light.

To confirm the effect of vanadium addition to the TiO_2 framework, the NH_3-TPD test was performed with the profiles shown in Fig. 8. These profiles have two parts: one that appears at temperatures of 100 to 150 °C, which is related to physical adsorption, and the other that appears at temperatures of 200 to 400 °C. In general, the low and high temperature peaks correspond to the weak and strong acid sites, respectively. For pure TiO_2, only one peak assigned to physical adsorption was found at around 100 °C, while a broad peak around 150-350 °C was observed in the V-TiO_2 sample. This indicates that vanadium generated new acid sites on the TiO_2 framework. In addition, a sharp peak appeared at 250 °C when the photocatalyst was impregnated with platinum species, and the strong acid sites were especially increased in Pt-V-TiO_2. This peak may be attributable to a hydrogen spillover of platinum.

Generally, photocatalysis is an oxidation-reduction reaction involving electrons and holes, and H_2-TPR experiments have been conducted to investigate the reduction behavior of catalysts. Fig. 9 shows the reduction profiles of the four particles. It has been suggested that Ti^{3+} is first reduced to Ti^0 at a lower temperature, while the higher temperature peak corresponds to the reduction of Ti^{4+} to Ti^0. Based on the TPR profile, the reduction of Ti^{3+} to Ti^0 was pre-

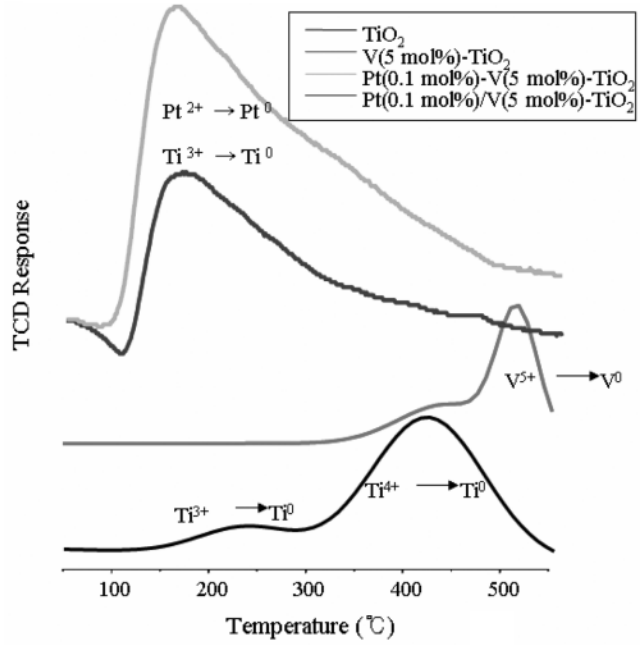

Fig. 9. H_2-TPR of nanometer-sized TiO_2, V-TiO_2, Pt-V-TiO_2, and Pt/V-TiO_2 photocatalysts.

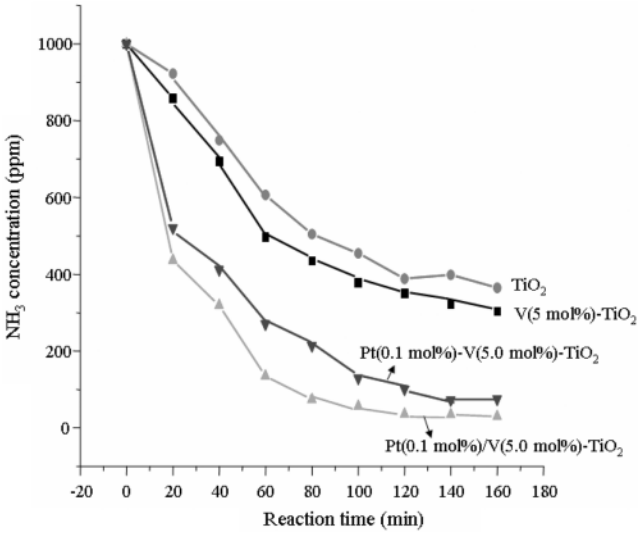

Fig. 10. Decomposition of highly concentrated ammonia over nanometer-sized TiO_2, V-TiO_2, Pt-V-TiO_2, and Pt/V-TiO_2 photocatalysts. Reaction conditions: ammonia concentration, 1,000 ppm; fixed catalyst weight on glass beads, 1.0 g; UV-light intensity, 365 nm; 24 W/m^2; batch system.

vented with V addition, while the reduction band of V^{5+} to V^0 appeared. For Pt-V-TiO_2 and Pt/V-TiO_2, a large band appeared at 150-200 °C, which was assigned to the reduction of Pt^{2+} to Pt^0. The intensity was particularly stronger in Pt-V-TiO_2. In general, a lower reduction temperature has a good influence on photocatalysis, but we could not find any such relationship in this experiment.

2. Decompositions of Ammonia over TiO_2, V-TiO_2, Pt-V-TiO_2, and Pt/V-TiO_2 Photocatalysts

Fig. 10 shows the photocatalytic performance for ammonia removal over the four photocatalysts in a batch photoreactor. Ammonia at 700 ppm was removed over pure TiO_2 after 160 min and the removal rate was slightly increased with vanadium addition. However, 1,000 ppm of ammonia was not completely removed after 160 min in V-TiO_2. Compared to V-TiO_2, the ammonia decomposition was remarkably enhanced with platinum addition, especially so in Pt/V-TiO_2 for which the ammonia was completely removed after 160 min. This result confirmed that the platinum-added V-TiO_2 has a better effect on the photodecomposition of concentrated ammonia.

On the other hand, however, during the conversion to N_2 about 5-30% of the ammonia was converted into undesirable NO_2 and NO. We estimated the total amounts of NO and NO_2 produced by using GC and GC/MS analyses with the results summarized in Table 2. We found that the partially oxidized NO and NO_2 dominated over V-TiO_2 and pure TiO_2, respectively, while both molecules were reduced by Pt addition, and were especially so in Pt-V-TiO_2. The total amounts over pure TiO_2, V-TiO_2, Pt-V-TiO_2, and Pt/V-TiO_2 were

Table 2. Product distributions during ammonia photo-destruction with reaction time over nanometer-sized TiO_2, V-TiO_2, Pt-V-TiO_2, and Pt/V-TiO_2 photocatalysts

(a) Conversion to NO (ppm)

Photo-catalysts Destructed time (min)	TiO_2	V(5 mol%)-TiO_2	Pt(0.1 mol%)-V(5 mol%)-TiO_2	Pt(0.1 mol%)-V(5 mol%)-TiO_2
20	44	85	17	36
60	31	72	21	32
100	29	57	18	21
140	18	43	15	20

(b) Conversion to NO_2 (ppm)

Photo-catalysts Destructed time (min)	TiO_2	V(5 mol%)-TiO_2	Pt(0.1 mol%)-V(5 mol%)-TiO_2	Pt(0.1 mol%)-V(5 mol%)-TiO_2
20	194	173	36	27
60	226	208	25	23
100	240	261	21	16
140	248	268	10	15

266, 311, 25, and 35 ppm, respectively. Consequently, our results confirmed that the Pt component is very useful to remove ammonia by conversion into N_2 in a photocatalytic system, and that the effect is a little higher in Pt-V-TiO_2 than in Pt/V-TiO_2.

CONCLUSIONS

This study investigated the effect of Pt addition to V-TiO_2 for highly concentrated ammonia (1,000 ppm) photodecomposition. Pt components were introduced to the V-TiO_2 photocatalysts by using two methods: the common sol-gel and impregnation methods. The main results were as follows:

1. The observed XRD peaks were assigned to V_2O_5 at 19.5, 27.5 and 30.20° in V-TiO_2, and to Pt metals at 39.80°(111) in Pt/V-TiO_2. However, these peaks were not seen in Pt-V-TiO_2.
2. In the XPS determination, the Pt component of Pt/V-TiO_2 was identified as Pt^{2+} from the $Pt4f_{7/2}$ and $Pt4f_{5/2}$ bands at 73.6 and 77.4 eV, respectively. However, the band was shifted to a lower binding energy in Pt-V-TiO_2.
3. The H_2-TPR curves showed that the temperature of the reduction from Ti^{3+} to Ti^0 was decreased by Pt addition and that the area was larger in Pt-V-TiO_2 than in Pt/V-TiO_2.
4. In NH_3-TPD, it was confirmed that the medium acidic site was increased with Pt impregnation, while the strong acidic site was remarkably increased in Pt-V-TiO_2.
5. The NH_3 decomposition slightly increased with vanadium addition compared to that of pure TiO_2, and the decomposition was further enhanced with Pt addition. In particular, the NH_3 decomposition reached 100% over Pt/V-TiO_2 after 120 min. However, the ammonia conversion into N_2 was a little higher in Pt-V-TiO_2 than in Pt/V-TiO_2.
6. Consequently, when the catalyst has more acidity, the photocatalytic performance also has more and the photoactivity increases over more easily reduced catalyst.

ACKNOWLEDGMENT

This work was supported by Korea Research Foundation (KRF-2003-D00014), to whom the authors are very grateful.

REFERENCES

1. P. I. Riggan, R. N. Lockwood and E. N. Lopez, *Environ. Sci. Technol.*, **19**, 971 (1985).
2. Y.-H. Son, M.-K. Jeon, J.-Y. Ban, M. Kang and S.-J. Choung, *J. Ind. Eng. Chem.*, **11**, 938 (2005).
3. M. Kang, *Appl. Catal. B: Environ.*, **37**, 187 (2002).
4. J. H. Lee, W. S. Nam, M. Kang, G. Y. Han, M.-S. Kim, K. Ogino, S. Miyata and S.-J. Choung, *Appl. Catal. A: General*, **244**, 49 (2003).
5. S.-H. Park, S.-C. Lee, M. Kang and S.-J. Choung, *J. Ind. Eng. Chem.*, **10**, 972 (2004).
6. M.-K. Yeo and M. Kang, *Water Research*, **40**, 1906 (2006).
7. M. Kang, D.-H. Choi and S.-J. Choung, *J. Ind. Eng. Chem.*, **11**, 240 (2005).
8. N.-L. Wu, M.-S. Lee, Z.-J. Pon and J.-Z. Hsu, *J. Photochem. & Photobiol. A: Chem.*, **163**, 277 (2004).
9. Q. Liu, X. Wu, B. Wang and Q. Liu, *Materials Research Bulletin*, **37**, 2255 (2002).
10. J. Yu, X. Zhao, Q. Zhao and G. Wang, *Materials Chemistry and Physics*, **68**, 253 (2001).
11. J.-H. Jang, S.-C. Lee, D.-J. Kim, M. Kang and S.-J. Choung, *Appl. Catal. A: General*, **286**, 36 (2005).